THE JOURNAL OF COMPARATIVE NEUROLOGY 499:132–143 (2006)

Regulation of KCC2 and NKCC during Development: Membrane Insertion and Differences between Cell Types

LING-LI ZHANG, MARIE E. FINA, AND NOGA VARDI*
Department of Neuroscience, University of Pennsylvania School of Medicine, Philadelphia, Pennsylvania 19104-6058

ABSTRACT

The developmental switch of GABA's action from excitation to inhibition is likely due to a change in intracellular chloride concentration from high to low. Here we determined if the GABA switch correlates with the developmental expression patterns of KCC2, the chloride extruder K^+-Cl^- cotransporter, and NKCC, the chloride accumulator Na^+-K^+-Cl^- cotransporter. Immunoblots of ferret retina showed that KCC2 upregulated in an exponential manner similar to synaptophysin (a synaptic marker). In contrast, NKCC, which was initially expressed at a constant level, upregulated quickly between P14 and P28, and finally downregulated to an adult level that was greater than the initial phase. At the cellular level, immunocytochemistry showed that in the inner plexiform layer KCC2's density increased gradually and its localization within ganglion cells shifted from being primarily in the cytosol (between P1–13) to being in the plasma membrane (after P21). In the outer plexiform layer, KCC2 was detected as soon as this layer started to form and increased gradually. Interestingly, however, KCC2 was initially restricted to photoreceptor terminals, while in the adult it was restricted to bipolar dendrites. Thus, the overall KCC2 expression level in ferret retina increases with age, but the time course differs between cell types. In ganglion cells the upregulation of KCC2 by itself cannot explain the relatively fast switch in GABA's action; additional events, possibly KCC2's integration into the plasma membrane and downregulation of NKCC, might also contribute. In photoreceptors the transient expression of KCC2 suggests a role for this transporter in development. J. Comp. Neurol. 499:132–143, 2006.

Indexing terms: GABA switch; chloride cotransporters; ganglion cells; bipolar cells; photoreceptors; chloride homeostasis

When a chloride channel opens, chloride may enter or leave the cell. The direction of chloride current depends on the cell's chloride equilibrium potential (E_{Cl}) relative to its resting membrane potential (E_{rest}). Among chemicals that open chloride channels, GABA is the most common and directly gates the $GABA_{A/C}$ chloride channel. Although GABA's main action in adults is to hyperpolarize neurons, during development it depolarizes them. This provides an important source of excitation required for normal development (Ben Ari, 2001, 2002; Owens and Kriegstein, 2002). The timeline of GABA's development and its action on ganglion and amacrine cells has been thoroughly studied in ferret retina. In this system, long used as a model for development, GABA is detected as early as embryonic day (E)30, at which time it excites amacrine and ganglion cells (Karne et al., 1997; Fischer et al., 1998). By postnatal days (P)14–18, however, GABA's action switches from excitation to inhibition. This switch is likely due to a change in E_{Cl} during development (Fischer et al., 1998; Myhr et al., 2001; Zhang et al., 2005). However, the question that still remains is what sets the E_{Cl} in ferret retina at different developmental stages.

Maintaining $E_{Cl} < E_{rest}$ requires an intracellular chloride concentration ($[Cl^-]_i$) lower than passively distributed; this can only be achieved by active transport of

Grant number: NEI EY11105 (to N.V.).

*Correspondence to: Noga Vardi, 122B Anat-Chem Bldg., Department of Neuroscience, University of Pennsylvania School of Medicine, Philadelphia, PA 19104-6058. E-mail: noga@retina.anatomy.upenn.edu

Received 13 March 2006; Revised 31 March 2006; Accepted 17 May 2006
DOI 10.1002/cne.21100
Published online in Wiley InterScience (www.interscience.wiley.com).

TABLE 1. Antibody List

Protein	Species, antigen, clone[1]	Host	Source of antibody (catalog number)	Dilution[2]
NKCC	Human (T4; recognizes NKCC1 + NKCC2)	Mouse monoclonal	Hybridoma Bank, Iowa City, IA	1:500
NKCC1	Mouse CT, aa 938-1011	Rabbit polyclonal	E. Delpire, Nashville, Tennessee (Plotkin et al. 1997)	1:20-1:150
KCC2	Rat CT, 112 last aa	Rabbit polyclonal	Cell Signaling Solutions, Lake Placid, NY	1:300
Synaptophysin	Bovine brain; vesicular fraction (Sy38)	Mouse monoclonal	Chemicon International, Temecula, CA (YM-9013)	1:60
Calbindin	Bovine kidney (CB-955)	Mouse monoclonal	Sigma, St Louis, MO (C 9848)	1:200
Recoverin	Bovine Purified whole protein	Rabbit polyclonal	Alexander Dizhoor, Pennsylvania College of Optometry, Elkins Park, PA; code: P26	1:500
PKC	Rat CT variable region	Rabbit polyclonal	Sigma, St Louis, MO (P 4334)	1:1,000
GABA	GABA coupled to KLH	Guinea pig	Chemicon International, Temecula, CA (AB175)	1:2,000
VGlut1	Rat CT-ygathstvqpprpppprdy	Guinea pig	Chemicon International, Temecula, CA (AB5905)	1:500

[1]Clone name given in parentheses.
[2]Dilution is for immunocytochemistry; for Western blots, antibody was 10 times more dilute.
CT, C-terminus.

chloride *out of* the cell. Conversely, maintaining $E_{Cl} > E_{rest}$ requires active transport of chloride *into* the cell. Such active transport may be achieved by cation chloride cotransporters or bicarbonate/chloride exchangers. A common mechanism to *extrude* chloride from a cell is to cotransport it with potassium using the outward potassium gradient. Of the four known isoforms of K^+-Cl^- cotransporter, the primary candidate in neurons is KCC2 (Payne et al., 1996). In many brain regions and in rat retina, KCC2 upregulates during development and supposedly follows a timeline similar to the GABA switch. In adults, KCC2's role as a chloride extruder is further supported by its broad localization to GABA-receptive neurons (Payne et al., 1996; Lu et al., 1999; Karadsheh and Delpire, 2001; Li et al., 2002). A common mechanism to *accumulate* chloride in a cell is to cotransport it with sodium. Of the two known isoforms of Na^+-K^+-Cl^- cotransporter, NKCC2 is thought to be specific to kidney and NKCC1 is currently the primary candidate for a neuronal accumulator (for review, see Russell, 2000). In several brain regions NKCC1 mRNA and protein are high early in development and downregulate with age (Plotkin et al., 1997b; Kanaka et al., 2001; Li et al., 2002; Mikawa et al., 2002; Ikeda et al., 2003). Moreover, in several cell types in adults NKCC1 localizes to neurons known to maintain high intracellular chloride, such as olfactory receptor neurons and retinal horizontal cells (Vardi et al., 2000; Reisert et al., 2005).

In this study we assessed the possible function of NKCC and KCC2 in the developing ferret retina by determining their expression relative to synaptophysin expression (as a measure of synaptic density) and by localizing KCC2 at the cellular and subcellular level. Our results are consistent with the idea that NKCC1 accumulates chloride while KCC2 extrudes it, and they show that KCC2 shifts from the cytosol to the plasma membrane around the time of GABA switch. The results further show a transient expression of KCC2 in photoreceptor, suggesting a role in maturation.

MATERIALS AND METHODS

Western blotting

Ferrets at P0–6 were deeply anesthetized with halothane and sacrificed by decapitation. Older ferrets were deeply anesthetized with ketamine (85 μg/gm) and xylazine (13 μg/gm, intraperitoneal injection) followed by anesthetic overdose. Animals were treated in compliance with federal regulations and University of Pennsylvania policy. After enucleation, a retina was cleaned of vitreous, detached from the pigment epithelium, frozen in liquid N_2, and stored at −80°C. Retinas were collected from animals at the following ages: litter A: P6, 9, 11, 14, 17, 23, 30, adult; litter B: P8, 10, 13, 15, 17, 28, 37, adult. Retinas from the same litter were processed in parallel. They were homogenized in 0.2–1 mL ice-cold homogenization buffer (5 mL per g wet weight) (in mM: 320 sucrose, 5 Tris,5 Tris-HCl, and 2 EDTA, 2.5 β-mercaptoethanol, pH adjusted to 7.4 at room temperature) containing protease inhibitor cocktails (P8340; Sigma Aldrich, St. Louis, MO). To produce crude membrane fractions, the homogenates were centrifuged at 6,000*g* for 10 minutes at 4°C, and the supernatant was centrifuged again at 50,000*g* for 45 minutes at 4°C in an Eppendorf centrifuge (5414C; Brinkman, Westbury, NY). The final pellet was resuspended in homogenization buffer and stored at −80°C. The protein concentration was determined using a Bio-Rad (Hercules, CA) protein assay.

Equal amounts of protein (10 μg) from each age of one developmental series were mixed with NuPAGE LDS sample buffer (Invitrogen, Carlsbad, CA), incubated for 45 minutes at 37°C, then loaded onto 5.0% or 7.5% Tris-glycine gel (Bio-Rad). Electrophoresis was performed with a mini-protean II electrophoresis cell (Bio-Rad) under reduced denaturing conditions. The resolved proteins were transferred to a polyvinylidene difluoride (PVDF) membrane (Bio-Rad) in transfer buffer (192 mM glycine, 25 mM Tris-Cl, pH 8.3, and 20% methanol) for 40–50 minutes at 15 V using a Bio-Rad Trans-Blot semi-dry transfer cell. The membrane was blocked with 5–7% skim milk in TBS-T (10 mM Tris-HCl, 150 mM NaCl, 0.1% Tween 20, pH 7.4) for 1 hour and incubated with the primary antibody overnight at 4°C in TBS-T-milk. After extensive washes the membrane was incubated with the secondary antibody conjugated to peroxidase in TBS-T-milk for 2 hours at room temperature. After extensive washes in TBS-T, bound antibody was detected by enhanced chemiluminescence (Pierce, Rockford, IL).

Quantification of Western blots

Chemiluminescence was captured within 20 minutes of the reaction using a Kodak Imaging Station 440CF system (with a 12-bit cool CCD camera) and was quantified using Kodak 1D (Sunnyvale, CA) imaging analysis software. Control experiments have shown that detection of protein is linearly proportional to the amount of protein in this assay. Exposures of each blot were adjusted to ensure that all signals were within the linear range. After subtracting background intensity from each pixel, we summed all the signals within a band to give the net band intensity. Because the proteins had an over a 1,000-fold difference in intensity between early and late retinas, in some highly expressing postnatal ages the protein smeared along the edge of the lane. We quantified the intensity of the smear and found it in most cases to be less than 3% of band intensity. This is less than the variability between samples, and thus could not affect the expression profile as presented in the figures. In experiments comparing NKCC and KCC2 expression in the same protein sample, we stripped membranes stained with one antibody with a stripping buffer (Pierce) and reprobed them with the second antibody. The transporter patterns detected with the second probes were similar to those with the fresh probes, but the detection sensitivity was reduced. Thus, only the freshly probed blots were included in our quantification. In experiments examining the expression of chloride transporters relative to synaptogenesis, we reprobed membranes (without stripping) with a monoclonal antibody against synaptophysin followed by antimouse IgG conjugated to peroxidase. This was feasible because the molecular weight of synaptophysin (38 kDa) is much lower than that of either transporter (above 140 kDa).

Immunostaining

Retinas were collected from ferrets at the following ages: litter 1: P3, 6, 10, 14, 18, 21, 25, adult; litter 2: P6, 8, 10, 13, 15, 17, 21, 28, 37, adult. Eyecups were immersion-fixed for 1 hour at room temperature in 4% paraformaldehyde and 0.01% glutaraldehyde diluted in 0.1 M phosphate buffer (PB) at pH 7.4, and cryoprotected with 30% sucrose in PB (overnight at 4°C). Eyes were then frozen in a mixture of Tissue Freezing Medium (Electron Microscopy Sciences, Fort Washington, PA) and 20% sucrose (1:2), then cryosectioned vertically in 10-μm sections. Cryosections were stained according to a standard protocol: soak in diluent containing 0.1 M PB, 10% normal goat serum, 5% sucrose, and 0.3% Triton X-100; incubate in primary antibody overnight at 4°C; and wash and incubate in secondary antibody for 3 hours at room temperature. Sections were mounted in Vectashield (Vector Laboratories, Burlingame, CA) and visualized with a confocal microscope (Leica, Nussloch, Germany). In double-labeling experiments, sections were incubated with a mixture of primary antibodies followed by a mixture of secondary antibodies. Primary antibodies and their specifications are listed in Table 1. Secondary antibodies were all from Jackson ImmunoResearch (West Grove, PA).

Quantification of immunostaining

Each developmental series was immunostained simultaneously under identical conditions and then imaged with a confocal microscope set to optimize for the strongest staining (to avoid saturation). Identical settings of objective lens, objective aperture, laser power, and photomultiplier gain/offset were then used for the whole series. For each postnatal day, three to nine areas (each 250 μm × 250 μm) were scanned from several sections for each postnatal day. Background was measured from an area outside the retinal tissue and subtracted from the mean intensity of the regions of interest. For presentation, all images of the same experiment used the same brightness and contrast adjustment (Adobe Photoshop, Adobe Systems, Mountain View, Ca). For graphing, the background-corrected mean intensity of the region of interest was normalized relative to the peak intensity. Contrast-enhanced images were used to estimate the intensity of KCC2-staining associated with the membrane relative to that in the cytosol. Cytosolic and membranal regions were circumscribed and the average intensity for each region was recorded. Average background intensity, taken from a nearby unstained region in the nerve fiber layer, was subtracted from each of these regions.

RESULTS

In ferret retina, GABA switches during P14–18 from exciting cells of the ganglion cell layer to inhibiting them (Fischer et al., 1998). Since this switch is likely due to a change in E_{Cl} of the cells, we examined the expression patterns of the putative chloride extruder KCC2 and the putative chloride accumulator NKCC from P3–37 and compared them to the adult patterns.

Specificity of antibodies

KCC2. Western blots of adult ferret retinal protein stained with the antibody against KCC2 showed two bands. In four blots the molecular weight of the lower band averaged 138 ± 8 kDa, consistent with the expected molecular weight of this transporter (Fig. 1A). The second band averaged 252 ± 8 kDa, but the low resolution of the molecular markers at this region did not permit determining whether this was a dimer or an aggregate of KCC2 with a different protein. Both bands appeared in the 50,000*g* pellet that corresponds to membrane fractions and were absent from the supernatant, consistent with functional KCC2 being a membrane-integrated protein. The immunostaining pattern of the adult ferret retina with anti-KCC2 resembles patterns in rat, rabbit, and monkey with staining strongly associated with the plasma membrane (Vu et al., 2000; Vardi et al., 2000, 2002) (see Figs. 5, 6). This staining was completely blocked by preabsorbing the antibody with its immunizing peptide. Thus, both Western blots and immunostaining indicate that the antibody against KCC2 is specific for ferret KCC2.

NKCC. We tested two antibodies against NKCC: a polyclonal antibody against NKCC1, the ubiquitous isoform of NKCC (Plotkin et al., 1997a), and the commonly used monoclonal antibody T4 that recognizes both NKCC1 and NKCC2 (Lytle et al., 1995; Vardi et al., 2000). The polyclonal antibody gave a single band at the expected size in Western blots of rat retinal protein, but it did not recognize NKCC1 in ferret kidney (Fig. 1B). In contrast, the T4 antibody gave a strong band that averaged 141 ± 5 kDa not only in rat retina but also in ferret kidney and retina (Fig. 1C,D). T4 also showed a possible dimer (256 ± 2 kDA) that was relatively strong in kidney and faint in

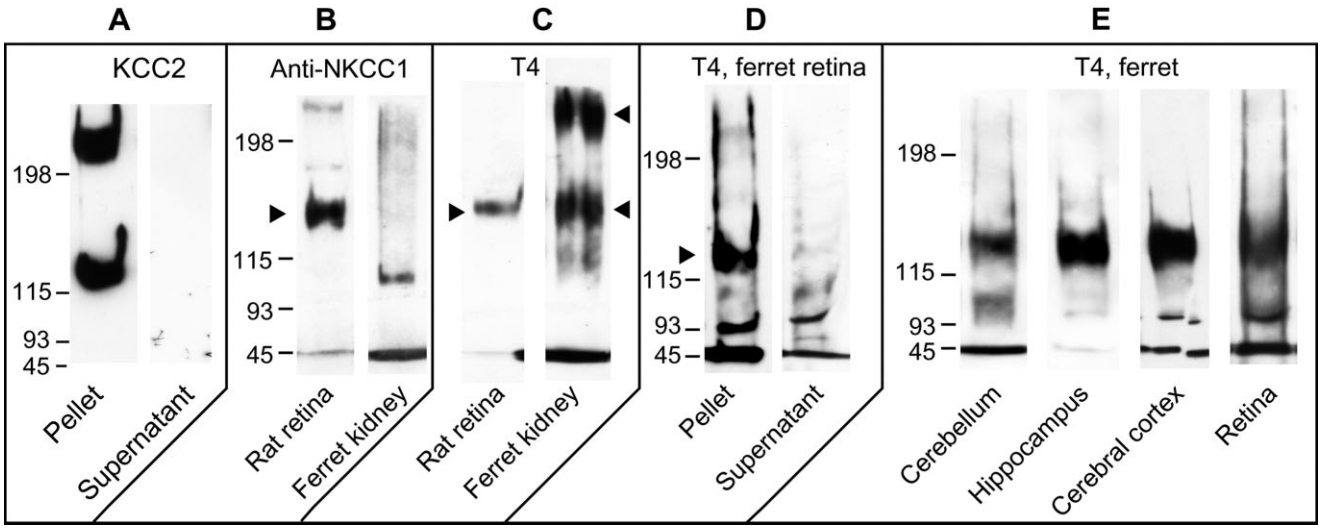

Fig. 1. Antibodies against rat KCC2 or human NKCC recognize the homologous ferret isoforms. **A:** Western blot of ferret retina probed with anti-KCC2 shows a monomer and a dimer in the pellet fraction but not in the supernatant. **B:** Western blots of rat retina and ferret kidney probed with polyclonal anti-NKCC1 antibody. The antibody recognized rat NKCC1 (arrowhead), but not ferret NKCC1. **C:** Western blots of rat retina and ferret kidney stained with the T4 antibody. The antibody recognized NKCC in both samples. While the retina showed only a monomer, the kidney showed also a dimer. **D:** Western blot of ferret retina probed with T4 antibody shows a band for retinal NKCC that is present in the pellet but not in the supernatant. **E:** Western blot of ferret brain regions probed with T4 shows that NKCC is also present in brain and retina. B and C are from the same blot, and A and D are from the same blot.

retina. In ferret retina the band was present only in the membrane fraction, consistent with NKCC being a membrane-integrated protein (Fig. 1D). Moreover, T4 gave a similar band for several other brain regions of ferret (Fig. 1E), suggesting that, as in rat, NKCC is widely expressed in ferret brain (Plotkin et al., 1997a). Nonetheless, in all these blots the T4 antibody recognized several nonspecific bands at lower molecular weights.

Immunostaining of adult ferret retina with T4 gave strong staining in the inner plexiform layer, but horizontal cells, which maintain high intracellular chloride and express NKCC1 in every species we have tested so far (monkey, rabbit, rat, mouse) (Vardi et al., 2000, 2002), did not stain. Moreover, this staining pattern of the inner plexiform layer was seen also in wildtype mice and NKCC1-null mice, indicating that T4 staining does not represent NKCC1 (unpubl. data). Thus, although the T4 antibody recognizes ferret NKCC in Western blots, it gives nonspecific immunostaining in the fixed ferret retina. Therefore, we limited our use of the T4 antibody to Western blots.

Expression of KCC2 increases monotonically during postnatal development

Western blotting with anti-KCC2 gave two bands throughout development, with the upper band usually being stronger than the lower band (Fig. 2). The expression level, quantified for each band separately, showed similar expression profiles, so the intensities of both bands were combined (Fig. 3A, five Western blots). KCC2 expression was detected at P10, maintained a relatively low level through P17, increased a little by P28, and peaked at the adult level. A plot of log intensity versus time revealed an exponential growth that had a time constant of 12.6 days and an increase from

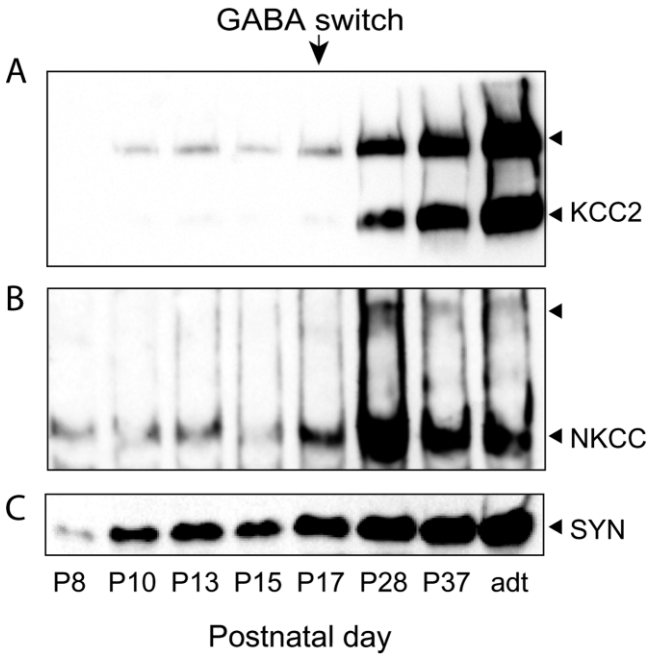

Fig. 2. KCC2 and NKCC have different expression patterns during development (Western blots). Western blots loaded with membrane fractions from different-aged ferret retinas were probed for KCC2 (**A**) and NKCC (with T4; **B**). After quantification the KCC2 blot was reprobed for synaptophysin (SYN; **C**). adt, adult.

P10 to adult of three orders of magnitude (Fig. 3B). As reference, synaptophysin, a ubiquitous component of synaptic vesicles, followed a similar exponential growth

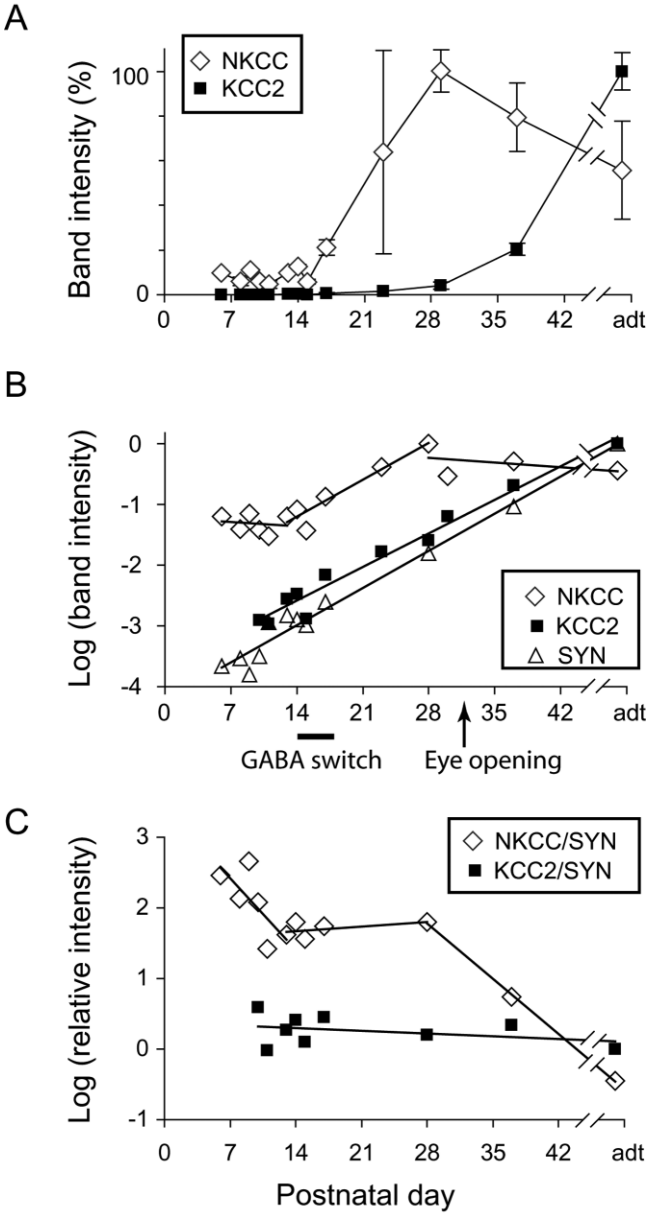

Fig. 3. Regulation of KCC2 and NKCC relative to synaptophysin. **A:** Quantity of KCC2 (average of five experiments) and NKCC (average of four experiments) from P6 to adult normalized to the peak expression of each transporter. Data are mean and standard deviation of the mean. **B:** Data replotted on a log scale shows an exponential increase in KCC2 and synaptophysin expression (SYN; three experiments). **C:** Plot of transporter to synaptophysin ratio shows that expression of KCC2 follows that of synaptophysin, while that of NKCC1 downregulates. Horizontal bar below x-axis shows time of GABA switch, arrow points to time of eye opening.

with a time constant of 11.4 days (three experiments, two series), suggesting that KCC2 protein synthesis increased with increasing synaptic density (Fig. 3B). Indeed, the ratio of KCC2 to synaptophysin stayed relatively constant during postnatal development (Fig. 3C).

Expression of NKCC peaks around eye opening

Western blotting with T4 gave a faint band in early retinas and a strong band later on, at which time a faint higher band (possibly a dimer) also appeared (Fig. 2B). Combining the intensities of the two bands in four experiments showed that NKCC's expression profile could be divided into three periods (Fig. 3). In the first period, prior to the development of the outer plexiform layer (P6–P14), NKCC maintained a stable low level. Since KCC2 and synaptophysin expression increased during this time, NKCC seems to downregulate relative to these two proteins. In the second period, when the outer plexiform layer grows quickly (P14–30), NKCC expression increased rapidly. This increase was exponential with a time constant (11.4 days) remarkably similar to that of KCC2 and synaptophysin. Thus, a similar mechanism, possibly the continuous formation of new synapses in this layer, may govern the addition of these proteins. In the final period, after eye opening (P32) NKCC expression declined. This contrasts with the continued increase in KCC2 and synaptophysin expression, suggesting that NKCC downregulates some time after the GABA switch.

KCC2 localizes to plasma membrane of amacrine and ganglion cells around the GABA switch time

Next we examined the developmental changes of KCC2 expression at the cellular and subcellular level. The P3 inner plexiform layer (the youngest retina tested) showed weak immunostaining for KCC2 (Fig. 4). At P10, when ganglion cell processes in this layer start to stratify, staining grew more intense. At P14 the staining distinguished two strata corresponding to the future ON and OFF sublaminas. At P18, the time of GABA's switch, the staining intensity reached about 40% of the adult level. In adult the entire inner plexiform layer was intensely stained, often masking laminar structure. Throughout development the average staining intensity in this layer followed a roughly linear increase up to the adult level (Fig. 4G).

The monotonic increase in KCC2 expression cannot explain the switch in GABA's action (see Discussion); therefore, we investigated the subcellular distribution of the staining. For KCC2 to be functional it must be inserted in a cell's plasma membrane. Indeed, in adult retina KCC2 staining of amacrine cell somas (somas with GABA staining) and ganglion cell somas (large somas devoid of GABA staining) was associated with the plasma membrane (Fig. 5). During development, staining for KCC2 began in the cytosolic region of the soma and gradually became associated with the plasma membrane. After P21, staining was practically restricted to near the plasma membrane (Fig. 6B,C). This shift was quantified by calculating the ratio of average pixel intensity associated with the plasma membrane to that of cytosolic staining (Fig. 6D). This ratio increased with age, first slowly until P13, then sharply, reaching a plateau at P21. The sharp increase around the time of GABA's switch suggests that insertion into the membrane plays an important role in activating KCC2.

Photoreceptors express KCC2 transiently before maturation

Staining for KCC2 was not detected in the neuroblast layer. At P18, very weak staining appeared in the top two

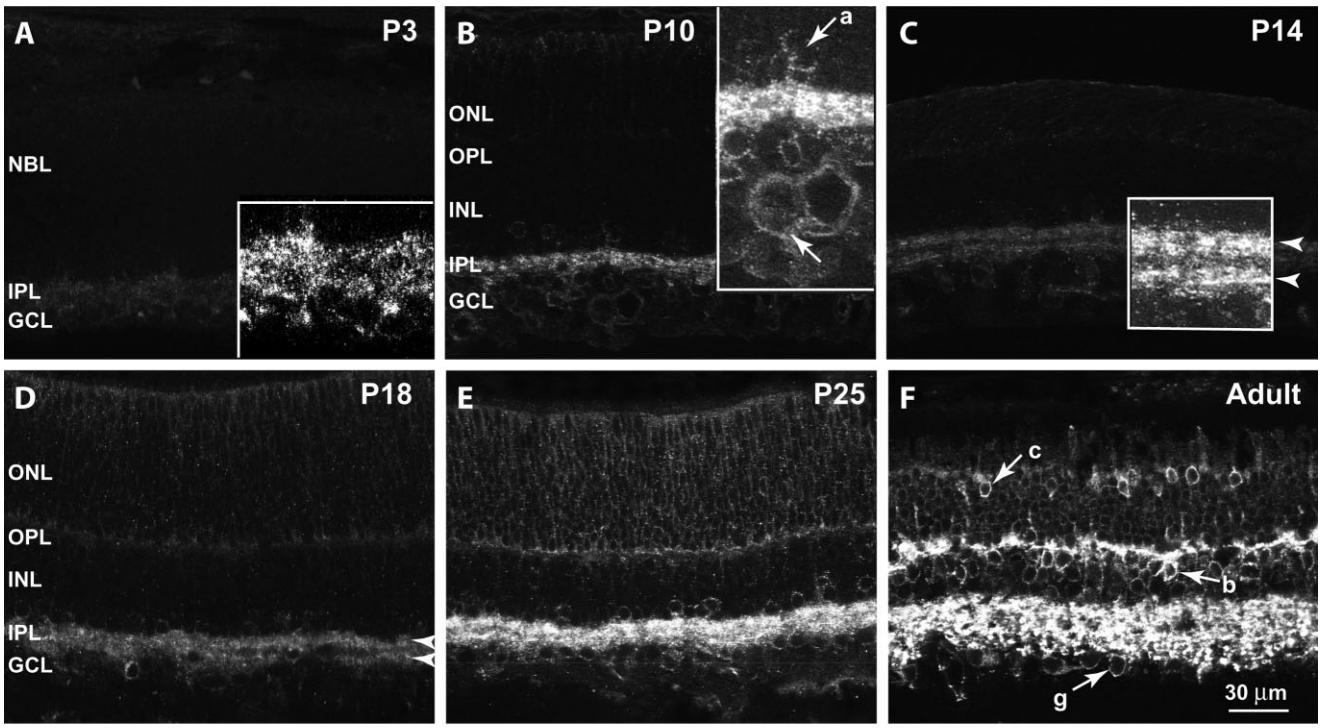

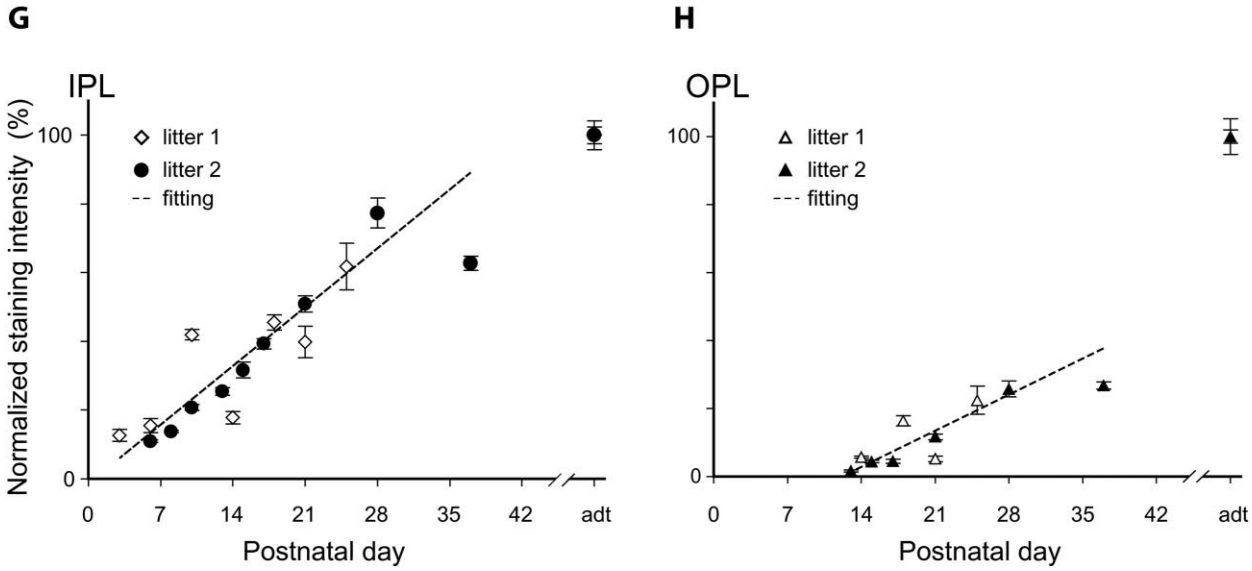

Fig. 4. KCC2 staining in the IPL and OPL increases during postnatal development. **A–F:** Confocal images of radial sections of ferret retina immunostained with anti-KCC2. Settings for image capture and presentation were kept constant across all postnatal ages. Insets show higher magnification with increased contrast to illustrate that staining is detected in the IPL at P3, in cell somas at P10 (arrows), and in two strata of the IPL at P14 (arrowheads). a, amacrine cell soma; g, ganglion cell soma; c, cone soma; b, bipolar cell soma; NBL, neuroblast layer; ONL, outer nuclear layer; OPL, outer plexiform layer; INL, inner nuclear layer; IPL, inner plexiform layer; GCL, ganglion cell layer. **G,H:** KCC2 expression during development quantified as average staining intensity per unit area in IPL or OPL normalized to adult level. Each data point is the average of 3–16 sections (mean ± SEM). Data from two litters were plotted independently. Combined data was fitted with a regression line (not using the adult (adt) data point).

to three tiers of what could then be identified as the outer nuclear layer (Fig. 4D). These stained somas probably correspond to newly differentiated cones and rods (Greiner and Weidman, 1981; Johnson et al., 2001). Between P25 and P37, all somas in the outer nuclear layer were weakly stained, but in adult only cone somas were stained. Staining in the outer plexiform layer also appeared at P18 and the intensity increased continuously

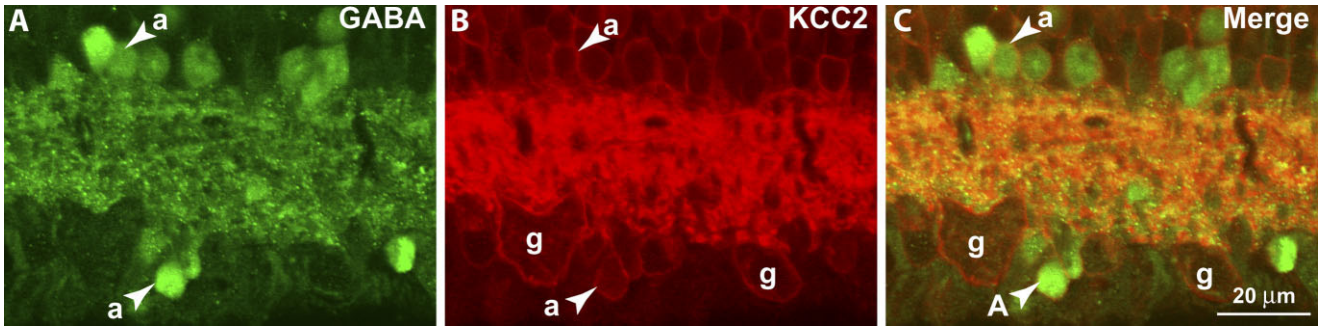

Fig. 5. KCC2 staining in adult localizes to plasma membrane of amacrine and ganglion cells. Double staining of adult ferret retina for GABA (**A**, green) and KCC2 (**B**, red). As in cat, where this antibody was established to be specific (Vardi and Auerbach, 1995), the guinea pig anti-GABA stains only amacrine cells (a). Ganglion cell somas (g) are large and unstained for GABA.

until adulthood, when it was comparable to that in the inner plexiform layer (Fig. 4H).

To determine whether the KCC2-stained structures in the outer plexiform layer were photoreceptor synaptic terminals, we double-labeled with synaptophysin. Synaptophysin is a synaptic protein that stains practically all presynaptic terminals, including photoreceptor terminals (Brandstätter et al., 1996; Reese et al., 1996). The staining pattern obtained in our samples was identical to published patterns and to what is expected from this protein. At P25 all structures that stained for synaptophysin also stained for KCC2, with little staining outside of these developing photoreceptor terminals (Fig. 7A–C). At P28 these photoreceptor terminals continued to stain, but KCC2 staining also appeared in certain structures beneath the terminals (Fig. 7D–F). In adult the terminals did not stain for KCC2, while the staining beneath them, presumably in bipolar cell dendrites, was strong (Fig. 7G–I). We also marked the photoreceptor synaptic terminals with a guinea pig antibody against the vesicular glutamate transporter vGlut1. In cat this antibody gave identical staining to that obtained by the established rabbit antibody, in which all photoreceptor (rod and cone) and bipolar terminals, and only those, were stained (Kao et al., 2004). Immunostaining was performed on sections of P25, P28, and P37, and the results were identical to those with synaptophysin (Fig. 8, shown only for P25). Importantly, staining for KCC2 at P25 was present in all photoreceptor terminals over very long stretches, suggesting both cone and rod terminals express KCC2 at this age. We conclude that KCC2 is expressed transiently in rod somas and in rod and cone terminals.

Bipolar cells express KCC2 after maturation

Immunostaining by a variety of antibody markers show that bipolar cells are well-formed by P28 (Miller et al., 1999). We confirmed the maturity of the cell's morphology in our litter by staining P28 retina for calbindin (localized to a subset of ON bipolar cells), recoverin (localized to a subset of OFF bipolar cells), and PKC (localized to rod bipolar cells). All of these types were well developed, projecting dendrites to the outer plexiform layer and axons to the correct sublaminas of the inner plexiform layer (Fig. 9A–C). However, these well-formed bipolar cells were virtually unstained for KCC2 even at P37 (Fig. 9D,E). In adult, KCC2 staining in bipolar cells increased markedly, showing strong staining in both somas and outer plexiform layer (Fig. 9F). This shows that bipolar somas express KCC2 relatively late, but it is still possible that other compartments of the cells express it earlier. In fact, in Figure 7 we observed that certain KCC2-stained structures in the outer plexiform layer of P28 retinas were not localized within photoreceptor terminals, suggesting that these were bipolar dendrites. Perhaps KCC2 in bipolar axon terminals develops even earlier. To test this possibility we labeled all bipolar terminals by immunostaining for vGlut1. This gave large terminals in sublamina 5 of the inner plexiform layer and smaller terminals throughout the inner plexiform layer. The large terminals likely belong to rod bipolar axon terminals. At P25, P28, and P37 the rod bipolar axon terminals were virtually unstained (Fig. 10, arrows). Only rarely did we observe a weak staining colocalized with vGlut1. In the adult all rod bipolar terminals were costained for KCC2, consistent with observations in rabbit and monkey (Vardi et al., 2000). Examining KCC2 staining in the smaller bipolar terminals was often hard because of their small size and the staining in the surrounding processes. Nonetheless, wherever these were well resolved they did not stain for KCC2 before P37 (Fig. 10, arrowheads). Even in the adult certain bipolar terminals remained unstained for KCC2. Thus, in contrast to photoreceptors, which express KCC2 before maturation, bipolar cells begin expressing KCC2 only after maturation, where the staining appears first in dendrites, then in somas, and finally in axon terminals.

DISCUSSION

Quantifying and localizing KCC2 in developing ferret retina revealed new information not previously reported in other species. First, during the first postnatal week, when the cells largely depolarize to GABA, KCC2 is expressed but is localized mainly to the cell's cytosol. Its insertion into the plasma membrane begins only after the second postnatal week, around the time when GABA switches from excitation to inhibition. Second, photoreceptor terminals, which do not express KCC2 in adulthood, do express this transporter transiently during their development.

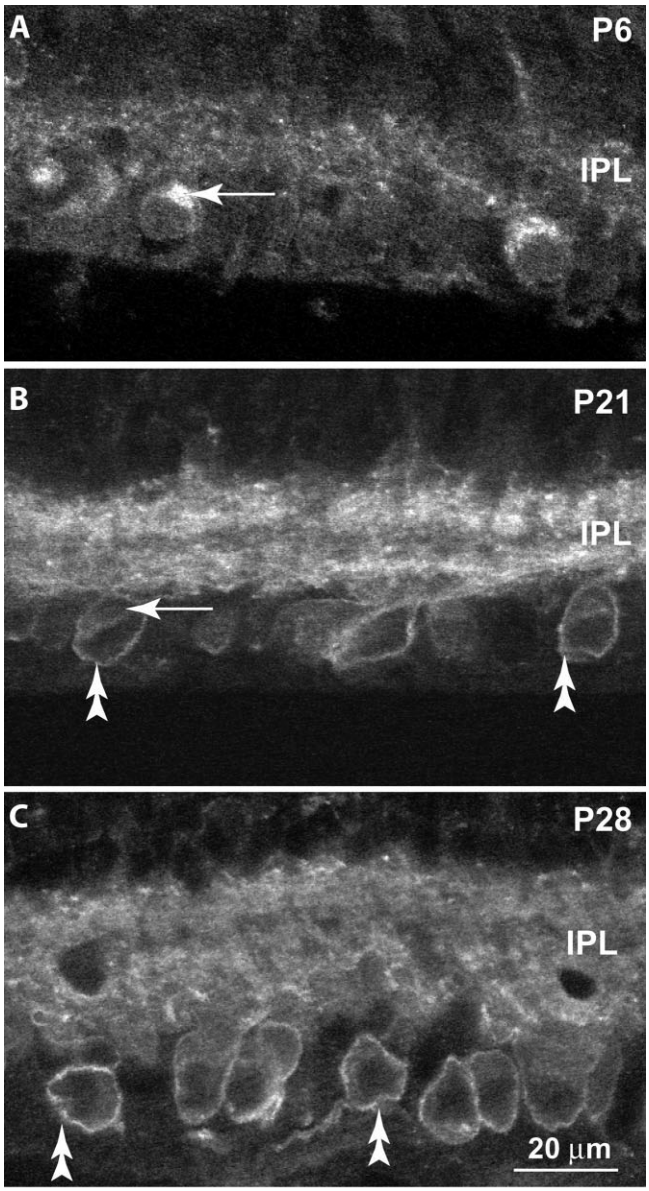

KCC2 is the main chloride extruder in neurons

In adult ferret retina we find that KCC2 localizes to amacrine, ganglion, and bipolar cells. This agrees with earlier observations in adult rat, rabbit, and monkey retinas, and is expected from the hyperpolarizing responses of these cells to GABA (Vardi et al., 2000, 2002; Vu et al., 2000). KCC2 was also present in somas of cone photoreceptors, but was absent from their axon terminals and from rods. If KCC2 extrudes chloride and lowers E_{Cl}, the two photoreceptor types should differ in their E_{Cl}. In salamander, at least, this holds true. Salamander cones maintain a more hyperpolarized E_{Cl} than rods (Thoreson et al., 2002, 2003; Thoreson and Bryson, 2004). Our data add to a large body of evidence supporting the hypothesis that KCC2 is the main chloride extruder in various neurons (Rivera et al., 1999; DeFazio et al., 2000; Gulacsi et al., 2003; Balakrishnan et al., 2003; Zhu et al., 2004).

Possible mechanisms underlying the developmental switch of GABA from depolarizing to hyperpolarizing

The switch cannot be fully explained by upregulation of KCC2. The switch of GABA's effect from depolarizing a cell to hyperpolarizing it in rat retina and other brain regions is often explained by upregulation of KCC2 (e.g., Vu et al., 2000; Stein et al., 2004). Since KCC2 is expressed mainly in the synaptic layers, upregulation as determined by Western blotting can be due to an increase in the volume of these layers relative to that of the nuclear layers, to an increase of synaptic density within the synaptic layers, or to both these changes. Such upregulation depends on growth, and does not indicate a qualitative change of function within an individual synapse.

We therefore evaluated growth-independent upregulation using two approaches. First, we estimated the amount of KCC2 relative to synaptophysin, a common synaptic protein, and thus a measure of synaptic density. Second, we quantified immunostaining of the inner plexiform layer across different ages to obtain a cleaner estimate of KCC2 density for this layer only. We found that upregulation of KCC2 during postnatal development resembles that of synaptophysin, suggesting KCC2 is added as new synapses are formed. Since KCC2 does not show a sudden increase in the inner plexiform layer at P14–18, the GABA switch time, its upregulation cannot explain the switch. Moreover, low expression of KCC2 before the

Fig. 6. KCC2 localizes to plasma membrane around switch time. **A–C:** KCC2 staining of somas in the ganglion cell layer at different postnatal ages. At P6 somatic staining was concentrated in the cytosol; at P21 staining in the cytosol was weak, while that of the plasma membrane was stronger; at P28 staining was restricted to the plasma membrane. Images were contrast enhanced to show the somas, so comparison of intensities is relevant only within a panel. Horizontal arrows point to cytosolic staining and double arrowheads point to plasma membrane. **D:** Ratio of average intensity in the plasma membrane relative to that in the cytosol across postnatal ages. Inset: demonstration of regions analyzed for the left cell in P21. The cytosol was circumscribed with a solid line and the membrane was denoted by the dotted annulus. Points are mean ± SEM; for P3 SEM is smaller than the symbol size. Number of cells are: P3, 48; P6, 103; P10, 26; P13, 37; P21, 27; P28, 63; adult, 19. Horizontal bar above the x-axis denotes time of switch.

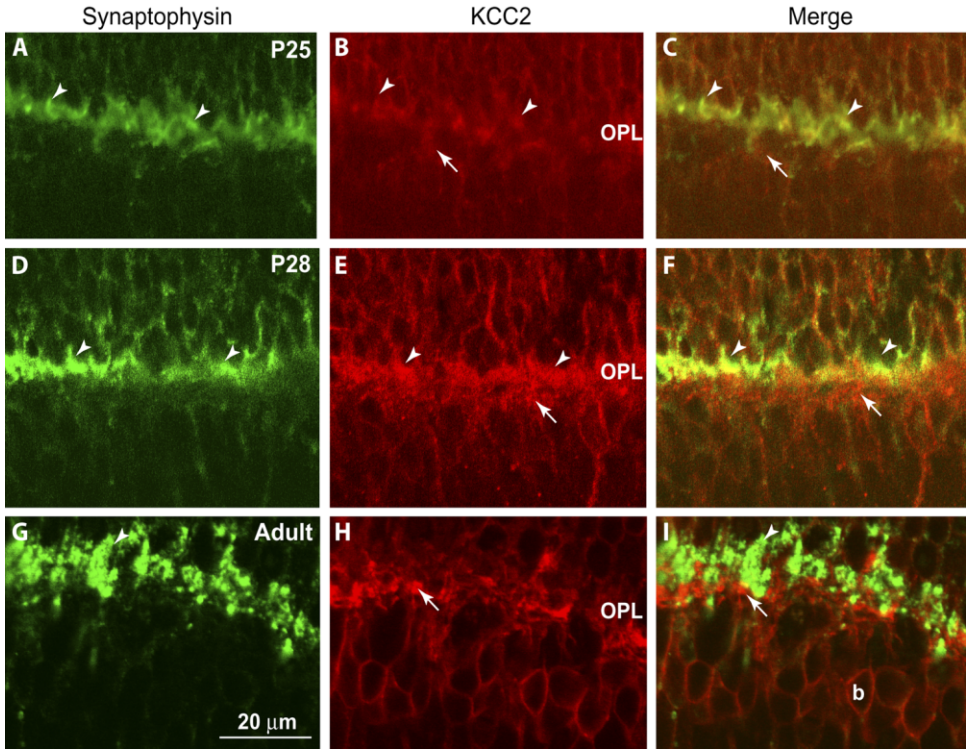

Figure 7

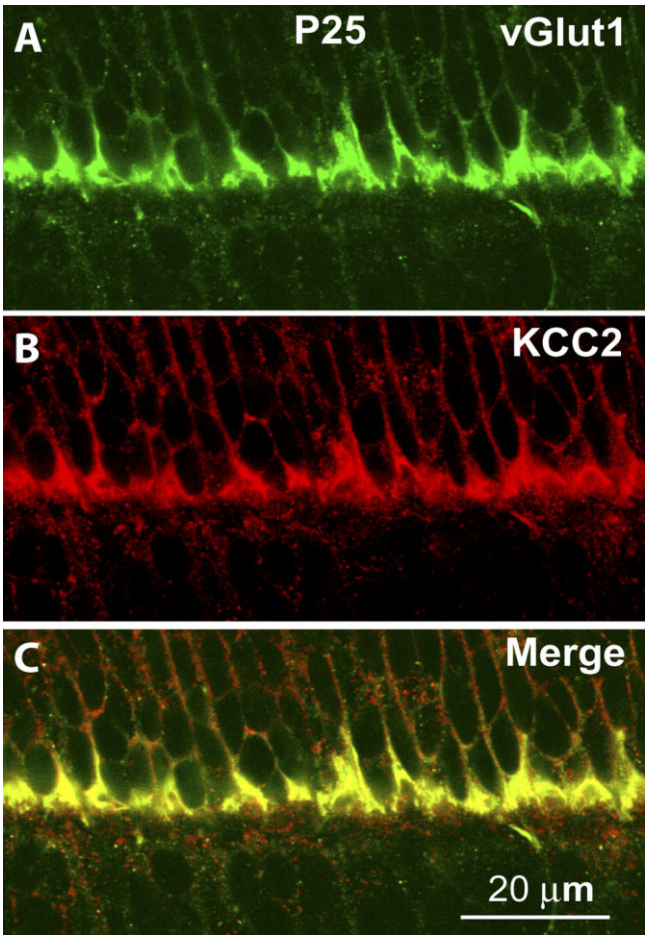

Figure 8

switch does not explain how neurons maintain relatively high intracellular chloride concentration, which is responsible for depolarization by GABA. Similar conclusions were drawn in the superior olive complex, where KCC2 was specifically expressed in cells that still depolarized to glycine (Lohrke et al., 2005).

NKCC may contribute to the switch. The intracellular chloride concentration in immature neurons is commonly attributed to the chloride accumulator NKCC1. Conceivably, if the accumulator is more active than the extruder, the net result will be accumulation of chloride. A dramatic decline in NKCC's expression during the switch could render KCC2 dominant thereafter. Our data show that NKCC was detected in immunoblots of membrane fractions before GABA's switch and before KCC2, possibly suggesting that it is active before KCC2. However, because the proteins were identified with different antibodies, the earlier detection of NKCC could simply result from a higher affinity of its antibody.

Although the relative activity of KCC2 and NKCC1 cannot be deciphered from the expression level, relative expression over time can still provide clues. In several brain regions NKCC1 clearly downregulates during development (Plotkin et al., 1997b; Marty et al., 2002), but in

Fig. 7. Photoreceptors express KCC2 transiently. Double staining for synaptophysin (green) and KCC2 (red) shows that, at P25, KCC2 staining was present primarily in synaptophysin-expressing photoreceptor terminals (arrowheads); at P28 it was also present below photoreceptor terminals (arrows); and in adult it was not localized to any synaptophysin-expressing terminals. b, bipolar soma.

Fig. 8. At P25 all photoreceptor terminals express KCC2. Double staining for vGlut1 (**A**, green) and KCC2 (**B**, red). Every terminal that stained with vGlut1 also stained for KCC2.

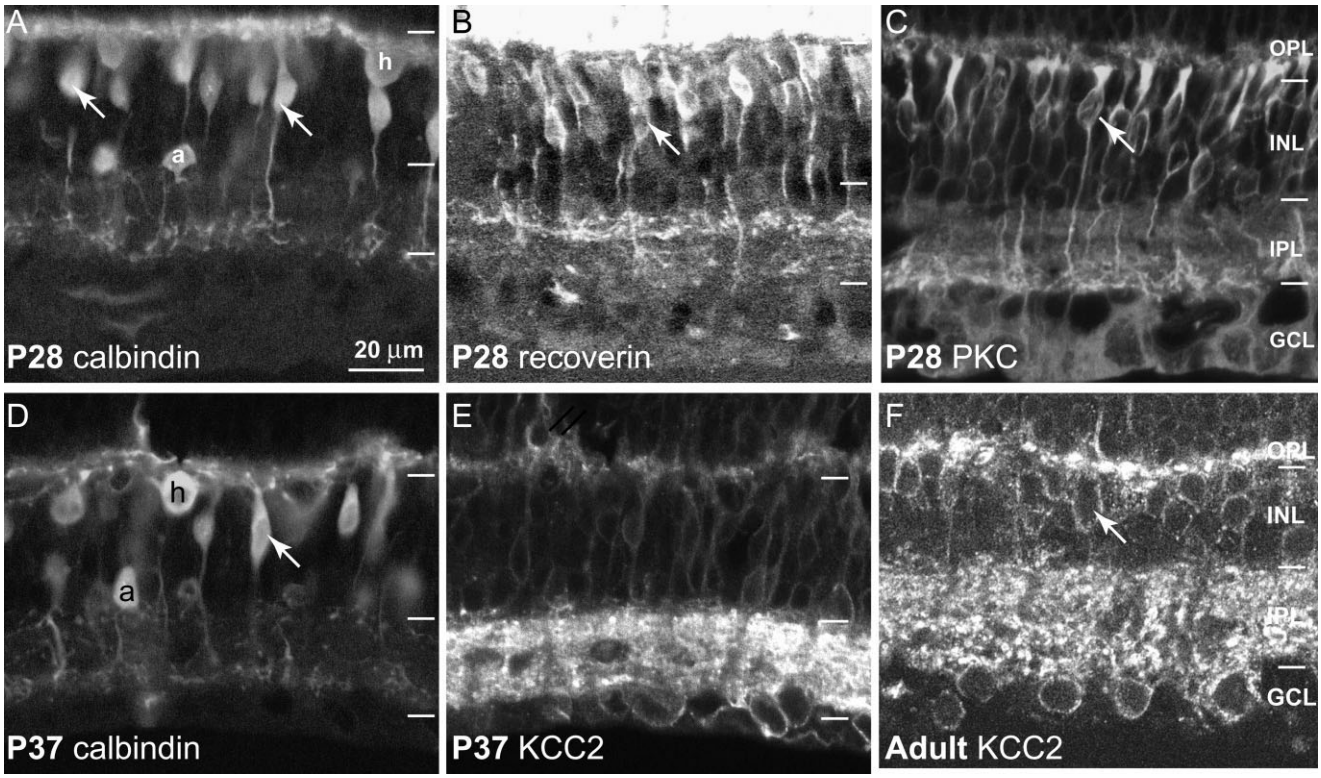

Fig. 9. Bipolar cell somas start to express KCC2 only after they are fully formed. **A–C:** Staining for calbindin, recoverin, and PKC show well-formed bipolar cell dendrites and axons at P28. Arrows point to bipolar cell somas. a, amacrine cell; h, horizontal cell. **D,E:** Double labeling for calbindin and KCC2 at P37 shows that, compared to ganglion cell somas, those of bipolar cells are still unstained or very weakly stained for KCC2. **F:** Staining for KCC2 in adult shows that bipolar cell somas (arrow) are now as strongly stained as ganglion cell somas.

retina NKCC's developmental profile is more complicated. Before GABA switches (P14), NKCC downregulates relative to synaptophysin, suggesting that NKCC is removed as new synapses are added. Between P14 to P28, the ratio of NKCC to synaptophysin becomes transiently flat; thereafter it resumes the declining trend.

The transient increase in NKCC expression (which parallels synaptophysin expression) between P14 and P28 coincides with the formation of the outer plexiform layer and maturation of horizontal cells that are known to express NKCC in adulthood (Greiner and Weidman, 1981; Vardi et al., 2000, 2002). The overall NKCC protein level in Western blots at this age likely reflects at least three simultaneously ongoing processes: the removal of NKCC from the mature synapse in the inner plexiform layer, the addition of NKCC in the immature synapse in the outer plexiform layer, and the addition of NKCC in the horizontal cells. To distinguish between these three contributions requires immunolocalization with a suitable antibody. Nonetheless, the overall decreasing trend of the ratio of NKCC to synaptophysin is consistent with a decline of this accumulator in the ganglion cells. Therefore, NKCC could contribute to the switch.

Timing of KCC2 integration into the plasma membrane may accelerate the GABA switch. The net activity of NKCC and KCC2 is determined not only by their relative expression level, but more importantly by the degree of their activation at each stage. For KCC2 to be active it has to be integrated into the plasma membrane. We assessed membrane integration from staining of amacrine and ganglion cell somas and found a predominantly cytosolic localization of KCC2 before P10, a mixed localization to cytosol and near membrane between P14–18, and a predominantly membranal-associated localization at P21 and later. This pattern correlates with Fischer et al. (1998), who described GABA's effect as excitatory between P1–11, inhibitory after P18, and mixed in effect in the interim. Thus, our data suggest that membrane integration might be a key step in activating KCC2 during the time of GABA switch, although they do not exclude additional events such as KCC2 phosphorylation.

Possible role of transient KCC2 expression in photoreceptors

Photoreceptors start to express KCC2 as soon as they are differentiated. In the outer nuclear layer staining is first apparent in the top tiers, where the first differentiated photoreceptor somas settle (Johnson et al., 2001). Also in the outer plexiform layer, staining is apparent as soon as this layer starts to form. This is in agreement with several brain regions where KCC2 is expressed as soon as neurons start to differentiate (Stein et al., 2004). Surprisingly, however, in photoreceptor terminals the expression is transient, since they do not express this isoform in the adult retina. The early KCC2 expression and its transient nature in photoreceptors suggest that, in addition to a role

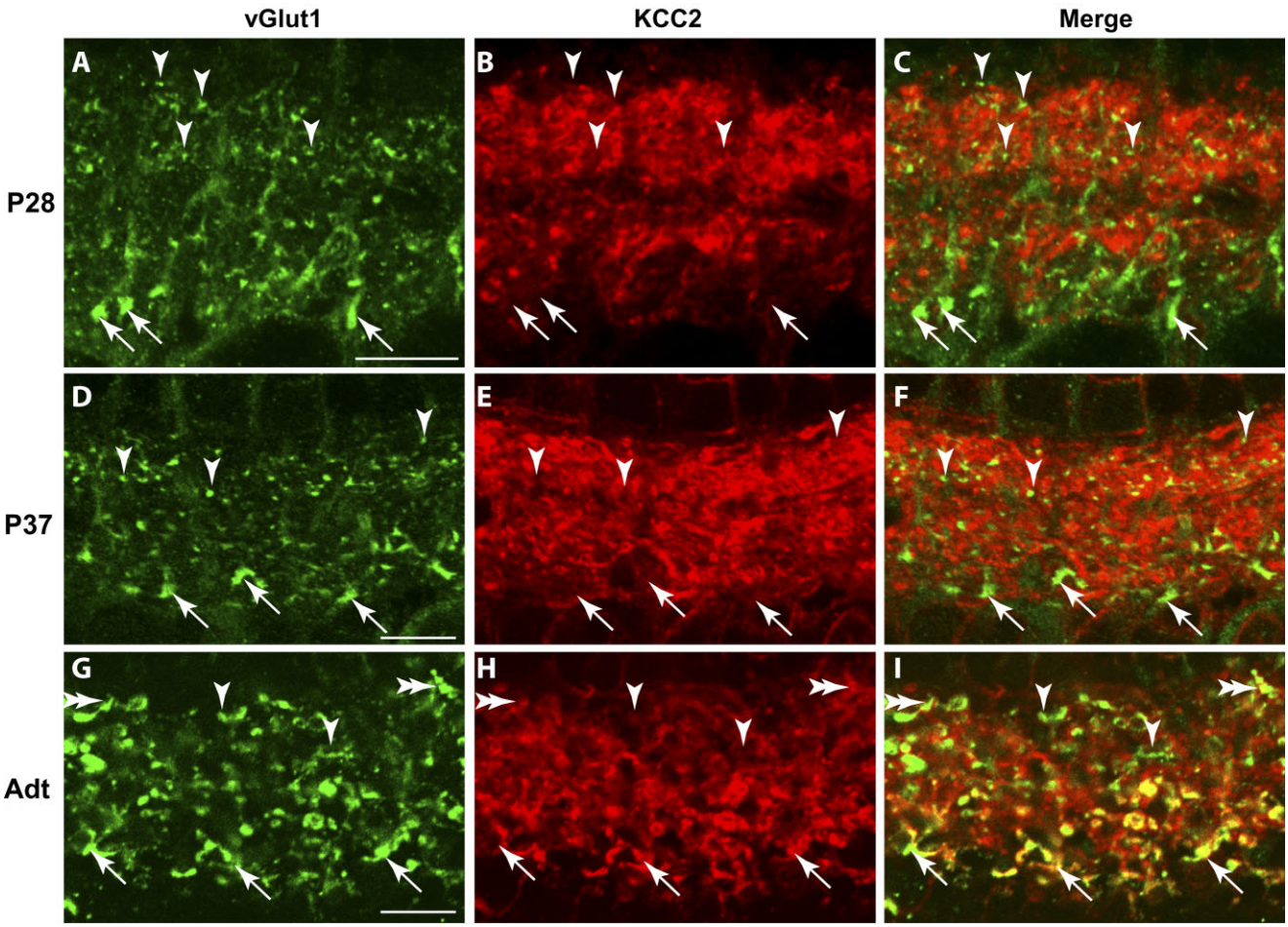

Fig. 10. Bipolar axon terminals do not express KCC2 before P37. Double staining for vGlut1 (green; **A,D,G**) and KCC2 (red; **B,E,H**) in the inner plexiform layer (IPL). Large terminal stained for vGlut1 in sublamina 5 (bottom of IPL) belong to rod bipolar cells (arrows). At P28 and P37 rod bipolar terminals were unstained for KCC2 (arrows on KCC2 panels point to unstained locations of the bipolar terminals). It was often difficult to resolve the small terminals (arrowheads), but when resolvable they were unstained for KCC2. At the adult (adt), rod bipolar terminals (arrows) and certain small terminals (double arrowheads) did stain for KCC2, but certain other small terminals did not (arrowheads). Confocal images were taken with a 60× objective, zoom 3 or 4, NA, 1.4. Scale bars = 10 μm.

in establishing a hyperpolarizing response to GABA, KCC2 might contribute to the process of maturation.

What is KCC2's role in the maturation of photoreceptors? KCC2 expression in photoreceptors coincides with synaptogenesis of the outer plexiform layer, elevated immunoreactivity for GABA and GAD_{67} in horizontal cells (unpubl. data), positive and transient immunoreactivity for $GABA_A$ receptor in photoreceptors (ferret: Karne et al., 1997; rabbit: Mitchell et al., 1999), structural development of photoreceptor outer segments, and expression of the cGMP-gated channel (Johnson et al., 2001). One possibility is that the constitutively active cGMP-gated channel causes hyperexcitability, and the $GABA_A$ receptor with the transient expression of KCC2 enables GABA to reduce this excitation. After P28, KCC2 ceases to be expressed in photoreceptors, possibly because this inhibitory balance is provided by light (eye opening is around P32), which hyperpolarizes photoreceptors. This hypothesis assumes that KCC2 is functional as soon as it is expressed so that it could counteract the activity of the cGMP-gated channel. However, evidence suggests that KCC2 is not functional during synaptogenesis of the outer plexiform layer as GABA elevates intracellular calcium in cone photoreceptors (Redburn, 1992; Huang and Redburn, 1996).

Since GABA and its depolarizing action is required for the normal development of cones and their synaptic triads (Redburn-Johnson, 1998; Huang et al., 2000), we consider the possibility that KCC2 builds up during the development of the outer plexiform layer and becomes active only after the cone synaptic triad has been formed. Such sudden action may be needed to put a brake on GABA's excitatory action in order to stabilize this complex synapse. Importantly, the $GABA_A$ receptor in photoreceptors is also expressed transiently, but for ferret retina it is not known when these receptors start to downregulate. Presumably, GABA's excitatory action could be stopped by the downregulation of the $GABA_A$ receptors, but this process may be slower than the activation of an already synthesized KCC2. The idea that KCC2 accumulates before it becomes active fits our observation in the inner retina, where ganglion cells express KCC2 long before GABA starts to hyperpolarize them. In this view, KCC2's role is

not only to establish the inhibition needed for the mature cell, but also to act quickly to stop developmental processes.

ACKNOWLEDGMENTS

We thank Peter Sterling and the Penn Neuroscience Graduate Group for continuing support, Dr. Rukmini Rao for reading the article, Dr. Eric Delpire for providing anti-NKCC1, and John Payne for providing the immunizing peptide for anti-KCC2.

LITERATURE CITED

Balakrishnan V, Becker M, Lohrke S, Nothwang HG, Guresir E, Friauf E. 2003. Expression and function of chloride transporters during development of inhibitory neurotransmission in the auditory brainstem. J Neurosci 23:4134–4145.

Ben Ari Y. 2001. Developing networks play a similar melody. Trends Neurosci 24:353–360.

Ben Ari Y. 2002. Excitatory actions of GABA during development: the nature of the nurture. Nat Rev Neurosci 3:728–739.

Brandstätter JH, Löhrke S, Morgans CW, Wässle H. 1996. Distributions of two homologous synaptic vesicle proteins, synaptoporin and synaptophysin, in the mammalian retina. J Comp Neurol 370:1–10.

DeFazio RA, Keros S, Quick MW, Hablitz JJ. 2000. Potassium-coupled chloride cotransport controls intracellular chloride in rat neocortical pyramidal neurons. J Neurosci 20:8069–8076.

Fischer KF, Lukasiewicz PD, Wong RO. 1998. Age-dependent and cell class-specific modulation of retinal ganglion cell bursting activity by GABA. J Neurosci 18:3767–3778.

Greiner JV, Weidman TA. 1981. Histogenesis of the ferret retina. Exp Eye Res 33:315–332.

Gulacsi A, Lee CR, Sik A, Viitanen T, Kaila K, Tepper JM, Freund TF. 2003. Cell type-specific differences in chloride-regulatory mechanisms and $GABA_A$ receptor-mediated inhibition in rat substantia nigra. J Neurosci 23:8237–8246.

Huang BO, Redburn DA. 1996. GABA-induced increases in $[Ca^{2+}]_i$ in retinal neurons of postnatal rabbits. Vis Neurosci 13:441–447.

Huang B, Mitchell CK, Redburn-Johnson DA. 2000. GABA and $GABA_A$ receptor antagonists alter developing cone photoreceptor development in neonatal rabbit retina. Vis Neurosci 17:925–935.

Ikeda M, Toyoda H, Yamada J, Okabe A, Sato K, Hotta Y, Fukuda A. 2003. Differential development of cation-chloride cotransporters and Cl^- homeostasis contributes to differential GABAergic actions between developing rat visual cortex and dorsal lateral geniculate nucleus. Brain Res 984:149–159.

Johnson PT, Williams RR, Reese BE. 2001. Developmental patterns of protein expression in photoreceptors implicate distinct environmental versus cell-intrinsic mechanisms. Vis Neurosci 18:157–168.

Kanaka C, Ohno K, Okabe A, Kuriyama K, Itoh T, Fukuda A, Sato K. 2001. The differential expression patterns of messenger RNAs encoding K-Cl cotransporters (KCC1,2) and Na-K-2Cl cotransporter (NKCC1) in the rat nervous system. Neuroscience 104:933–946.

Kao Y-H, Lassová L, Sterling P, Vardi N. 2004. Evidence that two types of retinal bipolar cell use both glutamate and GABA. J Comp Neurol. 478:207–218.

Karadsheh MF, Delpire E. 2001. Neuronal restrictive silencing element is found in the KCC2 gene: molecular basis for KCC2-specific expression in neurons. J Neurophysiol 85:995–997.

Karne A, Oakley DM, Wong GK, Wong RO. 1997. Immunocytochemical localization of GABA, $GABA_A$ receptors, and synapse-associated proteins in the developing and adult ferret retina. Vis Neurosci 14:1097–1108.

Li H, Tornberg J, Kaila K, Airaksinen MS, Rivera C. 2002. Patterns of cation-chloride cotransporter expression during embryonic rodent CNS development. Eur J Neurosci 16:2358–2370.

Lohrke S, Srinivasan G, Oberhofer M, Doncheva E, Friauf E. 2005. Shift from depolarizing to hyperpolarizing glycine action occurs at different perinatal ages in superior olivary complex nuclei. Eur J Neurosci 22:2708–2722.

Lu J, Karadsheh M, Delpire E. 1999. Developmental regulation of the neuronal-specific isoform of K-Cl cotransporter KCC2 in postnatal rat brains. J Neurobiol 39:558–568.

Lytle C, Xu JC, Biemesderfer D, Forbush B III. 1995. Distribution and diversity of Na-K-Cl cotransport proteins: a study with monoclonal antibodies. Am J Physiol 269:1496–1505.

Marty S, Wehrle R, Alvarez-Leefmans FJ, Gasnier B, Sotelo C. 2002. Postnatal maturation of Na^+,K^+,$2Cl^-$ cotransporter expression and inhibitory synaptogenesis in the rat hippocampus: an immunocytochemical analysis. Eur J Neurosci 15:233–245.

Mikawa S, Wang C, Shu F, Wang T, Fukuda A, Sato K. 2002. Developmental changes in KCC1, KCC2 and NKCC1 mRNAs in the rat cerebellum. Brain Res Dev Brain Res 136:93–100.

Miller ED, Tran MN, Wong GK, Oakley DM, Wong RO. 1999. Morphological differentiation of bipolar cells in the ferret retina. Vis Neurosci 16:1133–1144.

Mitchell CK, Huang B, Redburn-Johnson DA. 1999. $GABA_A$ receptor immunoreactivity is transiently expressed in the developing outer retina. Vis Neurosci 16:1083–1088.

Myhr KL, Lukasiewicz PD, Wong RO. 2001. Mechanisms underlying developmental changes in the firing patterns of ON and OFF retinal ganglion cells during refinement of their central projections. J Neurosci 21:8664–8671.

Owens DF, Kriegstein AR. 2002. Is there more to GABA than synaptic inhibition? Nat Rev Neurosci 3:715–727.

Payne JA, Stevenson TJ, Donaldson LF. 1996. Molecular characterization of a putative K-Cl cotransporter in rat brain. A neuronal-specific isoform. J Biol Chem 271:16245–16252.

Plotkin MD, Kaplan MR, Peterson LN, Gullans SR, Hebert SC, Delpire E. 1997a. Expression of the Na^+-K^+-$2Cl^-$ cotransporter BSC2 in the nervous system. Am J Physiol 272:173–183.

Plotkin MD, Snyder EY, Hebert SC, Delpire E. 1997b. Expression of the Na-K-2Cl cotransporter is developmentally regulated in postnatal rat brains: a possible mechanism underlying GABA's excitatory role in immature brain. J Neurobiol 20;33:781–795.

Redburn DA. 1992. Development of GABAergic neurons in the mammalian retina. Prog Brain Res 90:133–147.

Redburn-Johnson D. 1998. GABA as a developmental neurotransmitter in the outer plexiform layer of the vertebrate retina. Perspect Dev Neurobiol 5:261–267.

Reese BE, Johnson PT, Baker GE. 1996. Maturational gradients in the retina of the ferret. J Comp Neurol 375:252–273.

Reisert J, Lai J, Yau KW, Bradley J. 2005. Mechanism of the excitatory Cl^- response in mouse olfactory receptor neurons. Neuron 45:553–561.

Rivera C, Voipio J, Payne JA, Ruusuvuori E, Lahtinen H, Lamsa K, Pirvola U, Saarma M, Kaila K. 1999. The K^+/Cl^- co-transporter KCC2 renders GABA hyperpolarizing during neuronal maturation. Nature 397:251–255.

Russell JM. 2000. Sodium-potassium-chloride cotransport. Physiol Rev 80:211–276.

Stein V, Hermans-Borgmeyer I, Jentsch TJ, Hubner CA. 2004. Expression of the KCl cotransporter KCC2 parallels neuronal maturation and the emergence of low intracellular chloride. J Comp Neurol 468:57–64.

Thoreson WB, Bryson EJ. 2004. Chloride equilibrium potential in salamander cones. BMC Neurosci 5:53.

Thoreson WB, Stella SL Jr, Bryson EI, Clements J, Witkovsky P. 2002. D2-like dopamine receptors promote interactions between calcium and chloride channels that diminish rod synaptic transfer in the salamander retina. Vis Neurosci 19:235–247.

Thoreson WB, Bryson EJ, Rabl K. 2003. Reciprocal interactions between calcium and chloride in rod photoreceptors. J Neurophysiol 90:1747–1753.

Vardi N, Auerbach P. 1995. Specific cell types in cat retina express different forms of glutamic acid decarboxylase. J Comp Neurol 351:374–384.

Vardi N, Zhang LL, Payne JA, Sterling P. 2000. Evidence that different cation chloride cotransporters in retinal neurons allow opposite responses to GABA. J Neurosci 20:7657–7663.

Vardi N, Dhingra A, Zhang LL, Lyubarsky A, Wang TL, Morigiwa K. 2002. Neurochemical organization of the first visual synapse. Keio J Med 51:154–164.

Vu TQ, Payne JA, Copenhagen DR. 2000. Localization and developmental expression patterns of the neuronal K-Cl cotransporter (KCC2) in the rat retina. J Neurosci 20:1414–1423.

Zhang LL, Pathak HR, Coulter DA, Freed MA, Vardi N. 2005. Shift of intracellular chloride concentration in ganglion and amacrine cells of developing mouse retina. J Neurophysiol 94:2404–2416.

Zhu L, Lovinger D, Delpire E. 2004. Cortical neurons lacking KCC2 expression show impaired regulation of intracellular chloride. J Neurophysiol 93:1557–1568.